STRUCTURAL FEATURES OF FSW JOINTS OF METALS WITH DIFFERENT ELEMENT SOLUBILITY IN THE SOLID PHASE

G.M. GRIGORENKO, L.I. ADEEVA, A.Yu. TUNIK, S.N. STEPANYUK, M.A. POLESHCHUK and **E.V. ZELENIN**
E.O. Paton Electric Welding Institute, NASU
11 Bozhenko Str., 03680, Kiev, Ukraine. E-mail: office@paton.kiev.ua

Results of investigation of the structure and properties of dissimilar metal joints made by friction stir welding (FSW) are given. Systems with unlimited (Ni–Cu) and limited (Cu–Fe) solubility, as well as absence of component solubility (Al–Fe) in the solid state were studied. FSW of copper and nickel produced a sound welded joint with metal interpenetration to 3 mm depth. Mechanical mixing of metals plays the leading role in this process, whereas diffusion processes are negligible. Structure refinement occurs in mechanical mixing bands as a result of recrystallization processes. Copper diffusion into nickel along grain boundaries proceeds down to 20 μm depth with formation of interlayers of these metals solid solution. When studying the copper to steel welded joint, it was established that metal mixing has a leading role also in this process, and the role of diffusion processes is small. During welding a considerable grain refinement takes place both in the recrystallization zone, and in thermomechanically affected and heat affected zones. FSW of aluminium to iron resulted in formation of the joint zone of a considerable volume with aluminium penetration into iron down to 2.5 mm depth. Metal interaction proceeds here, namely mass transfer, primarily, of aluminum, and subsequent formation of Fe_2Al_7, $FeAl_2$ compounds. The hardest regions of welded joint zone contain intermetallics in the aluminium matrix. Such a structure has the hardness of 2870 ± 410 MPa that is more than 3 times lower than that of iron aluminides Results of the conducted investigations allow recommending this welding process to produce bimetal joints of dissimilar metals with different solubility of elements in the solid state. 20 Ref., 5 Tables, 15 Figures.

Keywords: *friction stir welding, welded joint, bimetal mechanical mixing of metals, diffusion, solid phase solubility, microstructure, X-ray microprobe analysis, elemental composition, microhardness*

Development of modern machine, car, aircraft, ship building and instrument making, as well as other industries, where mechanisms operate under extreme conditions, is impossible without application of new structural materials and dissimilar metal joints. These mostly are difficult-to-weld metallic materials, differing considerably from each other by their physico-mechanical properties. As a rule, when joining such metals, welding with an intermediate liquid phase leads to formation of structural complexes and phase components, which greatly lower joint performance. This problem can be solved using one of the solid phase welding processes, such as diffusion welding, magnetic-pulse, resistance without flashing, friction and explosion welding. All these processes allow solving many problems of resources and energy saving. They are applied in specific technologies, for instance, in manufacture of electric contacts, engine valves, transition pieces and other structures. This allows saving expensive materials, reducing structure weight, lowering power losses and, most importantly, joining difficult-to-weld materials.

One of the promising methods to join dissimilar metals and produce sound bimetal joints is friction stir welding (FSW) patented in 1991 by The Welding Institute [1]. Most of the studies point to numerous advantages of FSW, compared to other processes of producing permanent joints [2–7]: preservation of base metal properties in the welding zone to a considerable extent, compared to fusion welding processes; absence of harmful emissions or ultraviolet radiation during welding; possibility to produce defect-free welds in alloys, which in fusion welding are prone to formation of hot cracks and porosity in weld metal; no need for application of filler material or shielding gas; removal of surface oxides from the edges before welding; no losses of alloying elements in weld metal.

At present, possibility of FSW application for dissimilar metal welded joints is of great interest. Researchers [8, 9] demonstrated success in welding such dissimilar metals as aluminium and steel. FSW process to produce joints of aluminium to

magnesium was applied with success in works [10, 11]. Information on weldability and mechanical properties of dissimilar Al–Cu, Ni–Cu joints is given in [12–14]. As noted by the authors of these publications, the decisive role in weldability of dissimilar metals is played by metallurgical compatibility, determined by mutual solubility of metals being joined both in the liquid and in the solid state, as well as formation of brittle chemical compounds — the intermetallics.

The objective of this work is studying structural features and properties of bimetal joints with different solubility of components in the solid state, produced by FSW, in particular, Ni–Cu system, the components of which have unlimited solubility; systems with limited solubility (Cu–steel) and systems, in which solubility of metals being joined is absent in the solid state (Al–Fe).

Overlap welded joints were produced by FSW, the schematic of which is given in Figure 1.

Plasticizing and mixing of metals of the two plates occurs in a closed volume with application of a special rotating pin tool [14, 15], moving at a certain speed. Samples of initial alloys (copper, nickel, steel 3, aluminium and Armco-iron) were selected to conduct the FSW process. FSW modes and characteristics of materials being welded are given in Table 1.

A complex procedure was applied during investigations, including metallography (Neophot-32 optical microscope) and durometric analysis (LECO hardness meter M-400 at 0.249 and 0.496 N load). Electron studies of the structure and determination of its elemental composition by X-ray microprobe method (XRMM) were conducted in an analysis system consisting of JEOL scanning electron microscope JSM-35 CF (Japan) and X-ray spectrometer with dispersion by X-ray quantum energy (Oxford Instruments INCA Energy-350 model, Great Britain). A characteristic feature of this analysis is its locality — minimum excitation area is equal to 1 μm. One of the advantages of energy-dispersive spectrometer is the possibility of simultaneous analysis of about 50 elements (from boron to uranium) with

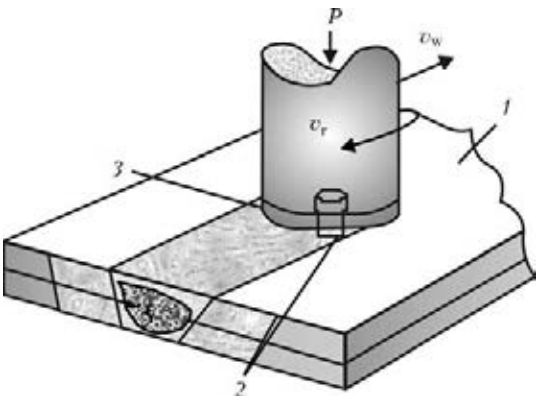

Figure 1. Schematic of FSW process: *1* — item; *2* — pin tool with special profile; *3* — shoulder; v_w — welding speed; v_r — rotation speed; P — applied load

reflection of the entire found spectrum. Structure image was obtained in secondary electron mode at $U = 20$ kV. To reveal the studied joint structure chemical reagents [16] and etching (Table 2) were used. To study the possibility of producing dissimilar joints, constitutional diagrams of Cu–Ni, Cu–Fe and Fe–Al binary systems were analyzed [17–19]. Microstructure of transverse and longitudinal sections of welded joints produced by FSW was studied. Phenomena of metal mixing in the plastic state, element diffusion, and conditions of intermetallic phase formation were studied, their composition and microhardness were determined.

Copper and nickel are two metals forming a continuous line of solid solutions (Figure 2) and having one-type crystalline lattices with close parameters (FCC). They belong to adjacent groups of periodic system (atomic radii differ by less than 10–15 %), and do not form any brittle intermetallics. In welding of these metals, joints with the most uniform properties are formed.

Cu–Ni constitutional diagram consists of three regions. In the upper part material consists of liquid solution of copper and nickel, in the middle region it contains both liquid and solid phases, the composition of which can be calculated using the lever rule. In the lower region Cu–Ni is substitutional solid solution, where copper and nickel atoms are irreplaceable in the crystalline lattice. Substitutional solid solution forms in Cu–

Table 1. FSW modes and welded material characteristics*

Material grade	Bimetal joint type	Layer thickness, mm	Pin tool immersion depth, mm	Layer microhardness, MPa	Welding speed, mm/min
N1/M0	Ni–Cu	4/10	5	2312/1160	40
M0/steel 3	Copper–steel	7/8	8	1160/2160	60
AMg6/008ZhR	Al–Fe	5/3	6	552/1260	60

*Pin tool rotation speed was 1250 rpm for all materials being welded.

Table 2. Reagents and conditions of metallographic etching

Material	Reagent composition	Application method	Remark
Cu (M0)	Nitric acid (50 ml) + water (50 ml)	Chemical etching at intensive stirring of reagent at τ = 5–30 s, T = 20 °C	Hydrochloric acid (80 ml) and water (20 ml) are used to remove oxide film at τ = 1–3 s, T = 20 °C
Ni (N1)	Ammonium sulphate (20 g) + water (100 ml)	Electrolytic etching at U = 6–15 V, τ = 3–10 s	Same
Steel 3	Nitric acid (4 ml) + ethyl alcohol (100 ml)	Chemical etching at τ = 5–30 s, T = 20 °C	Sample washing in ethyl alcohol
Al (AMg6)	Caustic soda (10 g) + water (100 ml)	Same	To remove oxide film hydrofluoric acid (50 ml) and water (50 ml) are used at τ = 1–3 s, T = 20 °C
Fe (008ZhR)	Nitric acid (4 ml) + ethyl alcohol (100 ml)	»	Sample washing in ethyl alcohol

Ni system, as copper and nickel solidify with FCC lattice formation, have similar atomic radii and electronegative valency [17, 18]. However, copper and nickel have different physico-mechanical characteristics. Copper is a soft, ductile material with high electrical conductivity, and melts at 1085 °C, while nickel is a relatively hard corrosion-resistant metal, which melts at 1455 °C.

Ni–Cu welded joint was produced at application of concentrated thermomechanical impact of the pin tool during FSW in the modes given in Table 1. Welding was performed through 4 mm nickel plate of N1 grade. Thickness of copper plate (M0 grade) was 10 mm.

Metallographic sections of this joint in the longitudinal and transverse direction were studied (Figures 3 and 4). Welded joint has no defects in the form of lacks-of-penetration, cracks or pores. An oval nugget of 4 × 6 mm size is observed in the transverse section of the joint zone (Figure 3, *a*, *b*), located in copper. It consists of concentrated deformation rings with nickel particle inclusions, their content being about 10 vol.%. In the nugget upper part a region of plastic displacement of nickel into copper formed as a result of pin tool impact through nickel. In this region of 2.5 × 3.0 mm size copper entrapment is found, its content reaching about 15 vol.%.

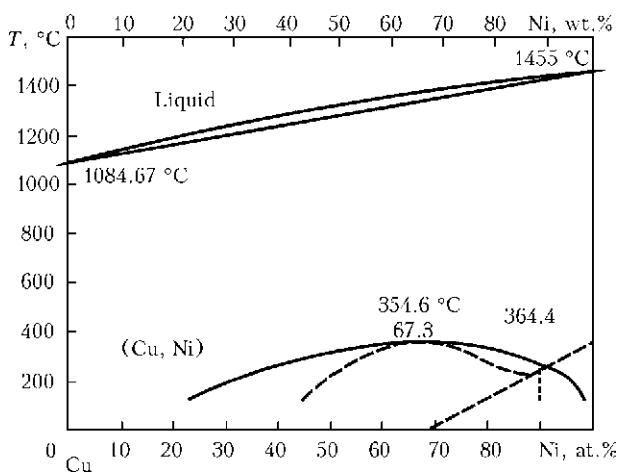

Figure 2. Constitutional diagram of Cu–Ni system [17]

When studying the longitudinal section, interpenetration of nickel and copper to the depth of down to 3 mm occurs in these metals joint zone. Metal mixing is observed in the form of interpenetrating alternating bands, oriented in the direction of pin tool movement (see Figure 4, *a*, *b*). Copper and nickel bands are equal to 0.3–0.6 and 0.03–0.30 mm, respectively. In these bands structure refinement takes place as a result of recrystallization processes. In copper grain size varies from 5 to 20 , and in nickel — from 5 up to 40 μm. Nickel band microhardness is equal to 1270 ± 40, and in copper it is 1140 ± 50 MPa. Above metal mixing region in nickel, a thermomechanically affected region of up to 3 mm length with oriented deformation bands (Figure 4, *a*, *c*) and grain size of 20 to 70 μm is found. Dark bands of deformed nickel feature a higher hardness (1610 ± 160 MPa), compared to light spaces between them (1290 ± 110 MPa). Edge region of nickel — HAZ, located above the thermomechanically affected zone, has coarser grains.

In copper a recrystallization region up to 0.6 mm wide with fine grain of 15–20 μm and up to 0.1 mm thermomechanically affected region with slightly deformed grain going into the base metal are observed under the mechanically stirred zone (see Figure 4, *d*). In both these regions, nickel inclusions are found in the form of elongated (spindle shaped) fragments with microhardness of 1300 ± 170 MPa.

Band edges and nickel regions directly contacting copper (Figure 4, *b*, *e*, *f* and Figure 5) are stronger etched out and have lower microhardness (1100 ± 60 MPa). This is attributable to copper and nickel interdiffusion along grain boundaries with formation of interlayers of these

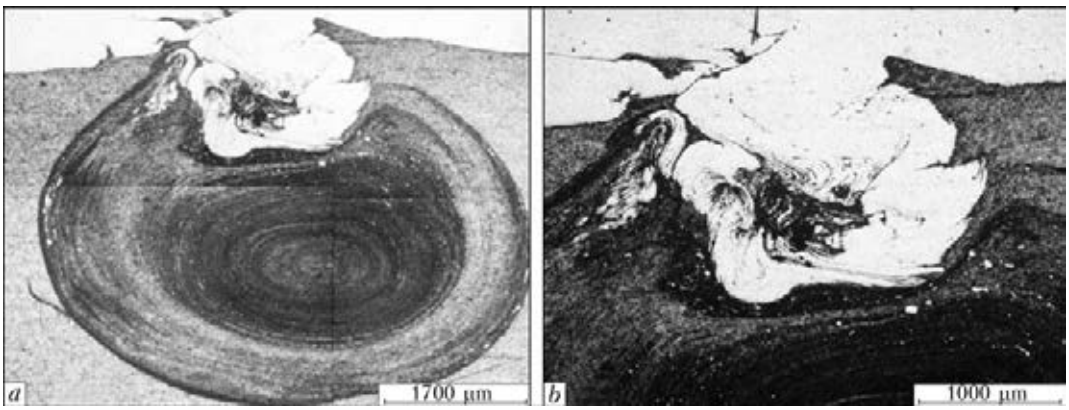

Figure 3. Microstructure of transverse microsection of Ni–Cu welded joint produced by FSW: *a* — general view; *b* — region of nickel mixing with copper

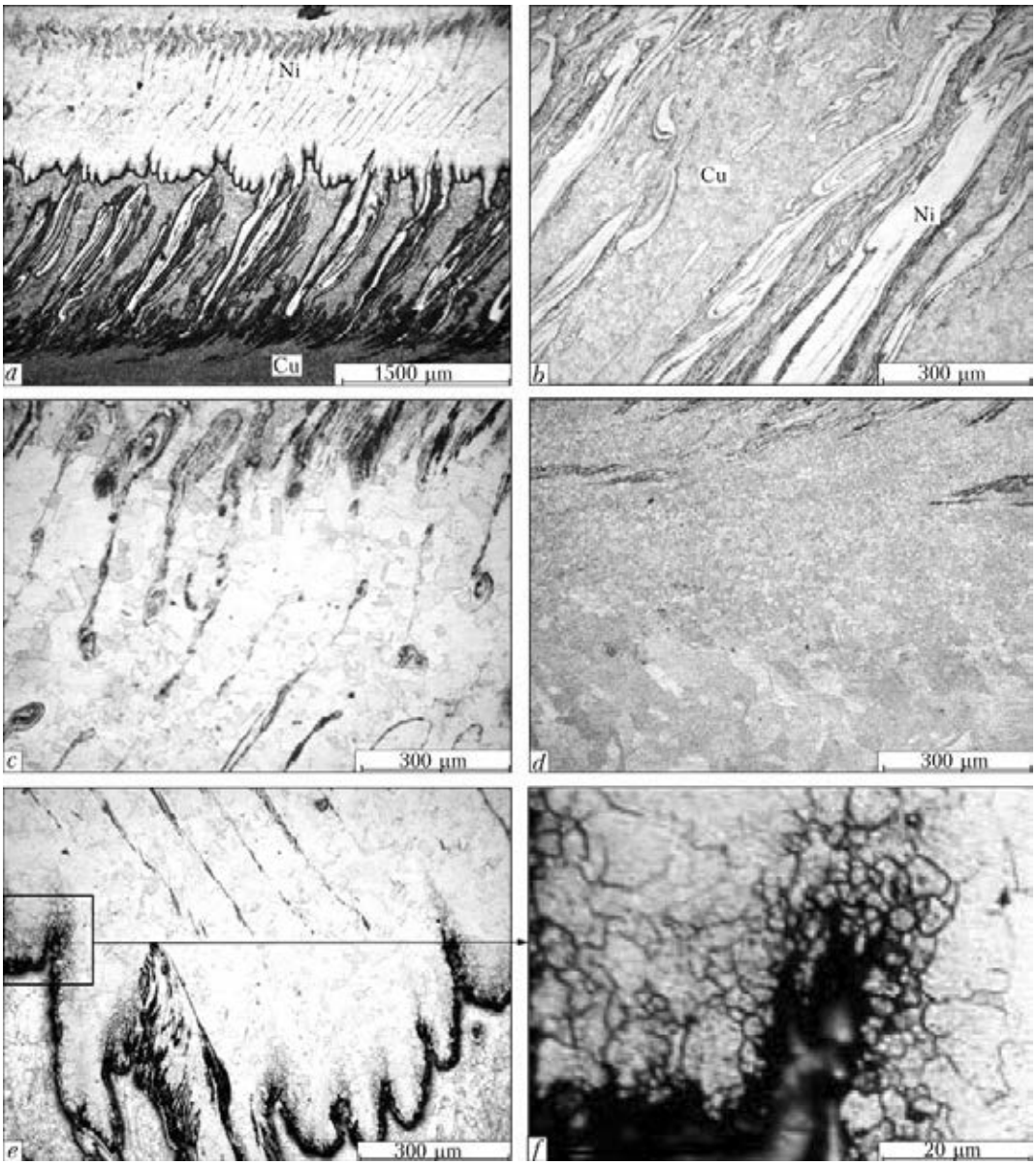

Figure 4. Longitudinal microstructure of Ni–Cu welded joint produced by FSW: *a*, *b* — zone of nickel mixing with copper; *c*, *d* — thermomecanically affected zone in nickel and copper, respectively; *e*, *f* — zone of copper interdiffusion in nickel

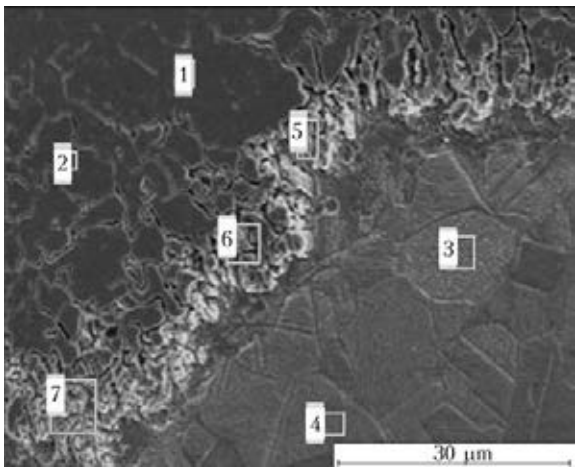

Figure 5. Microstructure of Ni–Cu contact zone filmed in secondary electrons (here and in Figure 6, *a* for numbers see Table 3)

metals solid solution (see Figure 4, *e*, *f*). XRMM method was used to analyze the composition of contact zone of the two metals, and it was established that copper diffusion into nickel to the depth of 10–20 μm takes place along grain boundaries.

When studying the joint zone in characteristic radiation, no significant interdiffusion of elements in-depth of alternating layers of nickel and copper was found. Figure 6 and Table 3 show the results of mapping the mechanically stirred zone of metals in Ni–Cu joint. Thus, investigation of nickel to copper welded joints showed that metal mixing in the plastic state plays the leading role in FSW processes with their interdiffusion being less important.

Copper–steel system was considered in order to study the possibility of producing by FSW joints of dissimilar metals with limited solubility of components in the solid state. According to Cu–Fe constitutional diagram, carbon solubility in copper is practically absent in the solid state, whereas in liquid state it is equal to 0.00015–0.003 wt.% at temperatures of 1100–1700 °C [17–19]. Carbon addition to Fe–Cu alloys somewhat lowers copper solubility in solid iron and does not change the overall pattern. Therefore, in order to analyze the process the authors considered the interaction between copper and iron. Constitutional diagram of Cu–Fe system is given in Figure 7. Data on complete or partial solubility of iron and copper in the liquid state are contradictory. The system shows three zones of primary crystallization of δ, γ and ε phases and three transformations (two peritectic and one eutectoid) proceeding at 1478, 1094 and 850 °C. Absence of delamination in Fe–Cu system is shown. It is, however, observed in overcooled condition (100 °C and more). Iron solubility in copper at 1025, 900, 800 and 700 °C is equal to 2.5, 1.5, 0.9 and 0.5 wt.%, respectively [19]. At further temperature lowering, iron solubility in copper changes only slightly. Pure copper has FCC lattice so that its addition widens the range of γ-iron. Copper solubility in γ-solid solution (8 wt.%) is higher than in α-solid solution (0.3 wt.%) and the ratios in this system are similar to Fe–C system. No intermetallics are found in this system.

Table 3. Composition of studied regions of Ni–Cu joint, wt./at.%

Studied region	Ni	Cu
Acc. to Figure 5		
1	100	0
2	100	0
3	0.30/0.32	99.70/99.68
4	0.37/0.40	99.63/99.60
5	75.46/76.90	24.54/23.10
6	91.64/92.22	6.36/7.78
7	83.92/84.95	16.08/15.05
Acc. to Figure 6, *a*		
1	99.23/99.29	0.77/0.71
2	99.18/99.24	0.82/0.76
3	4.03/4.35	95.97/95.65
4	5.96/6.42	94.04/93.58

FSW was performed on plates of copper and low-carbon steel (see Table 1). Pin tool impact

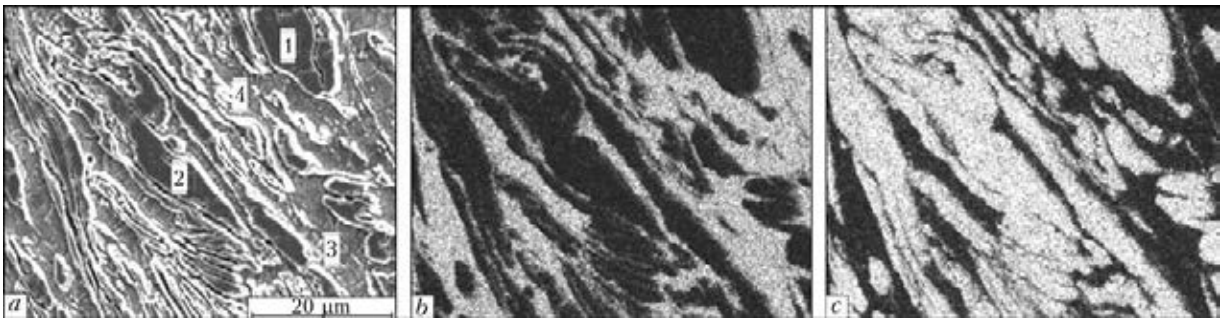

Figure 6. Image of Ni–Cu joint zone obtained in secondary electrons (*a*) and in characteristic radiation of copper (*b*) and nickel (*c*)

was applied through 7 mm copper plate. Investigation of transverse and longitudinal section of copper to steel welded joint showed that it has no defects: no cracks, lacks-of-penetration or pores were detected (Figures 8 and 9). It is found that in the longitudinal direction the joint is of serrated nature. In copper wedge-like intrusions are observed, which are inclined in the welding direction (Figure 8, *c*). Maximum depth of their penetration was equal to 500 μm. This region consists of finest steel particles of 1 to 10 μm size embedded into deformed copper, and microhardness of these zones is 2740 to 3020 MPa. Located above such wedge-like intrusions is incomplete recrystallization zone of copper — round-shaped grains of 30 to 100 μm size, chaotically located between copper base metal grains (Figure 8, *b*). Their maximum quantity equal to approximately 80 vol.% is in direct vicinity of the zone of joint with steel. Farther from the joint zone their quantity decreases, and their size becomes smaller. Extent of the zone of incomplete recrystallization in copper is equal to 600–800 μm.

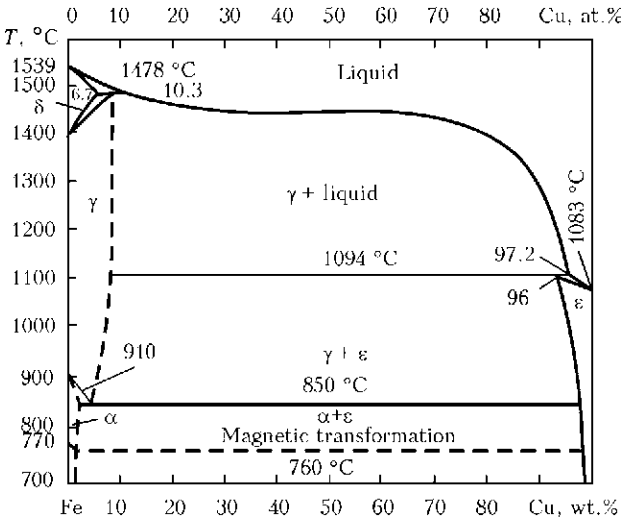

Figure 7. Constitutional diagrams of Cu–Fe system [19]

HAZ width in steel is equal to 4.5 mm. Zones of incomplete recrystallization, fine and medium grain are clearly visible (Figure 8, *c–e*). Medium grain zone is located directly in the zone of joint with copper. In the contact zone steel grain size is smaller by an order of magnitude than in the

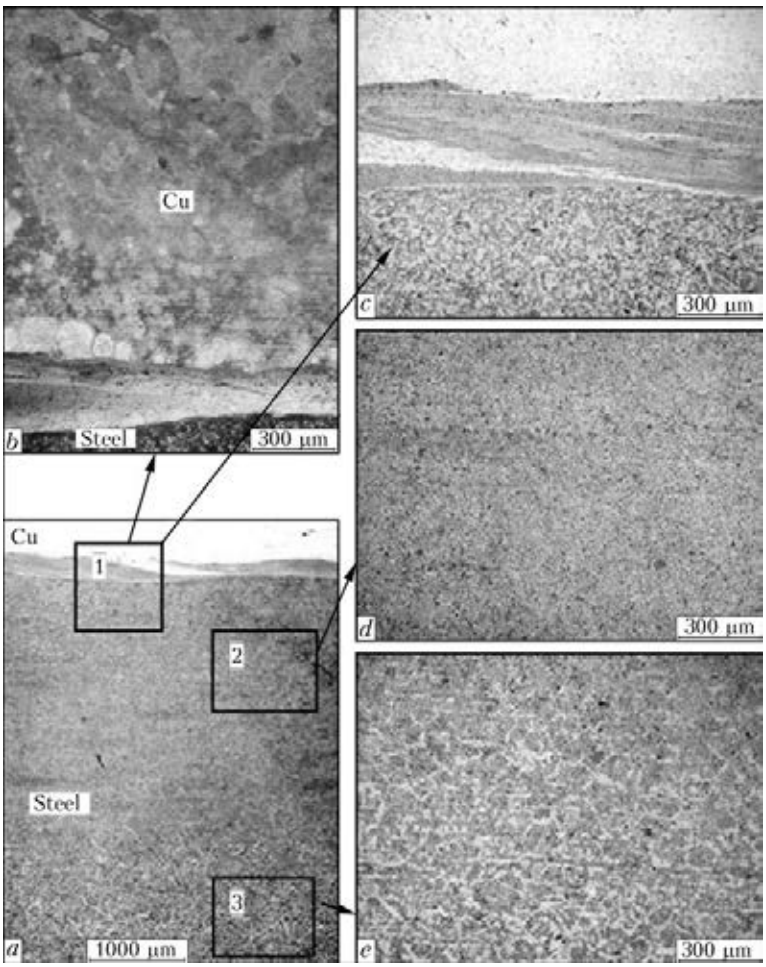

Figure 8. Longitudinal microstructure of copper–steel welded joint produced by FSW: *a* — general view of welded joint; *b* — zone of steel mixing with copper; *c* — medium grain region; *d* — fine grain region in steel HAZ; *e* — incomplete recrystallization zone in steel (here and in Figures 10 and 11, *a* for numbers see Table 4)

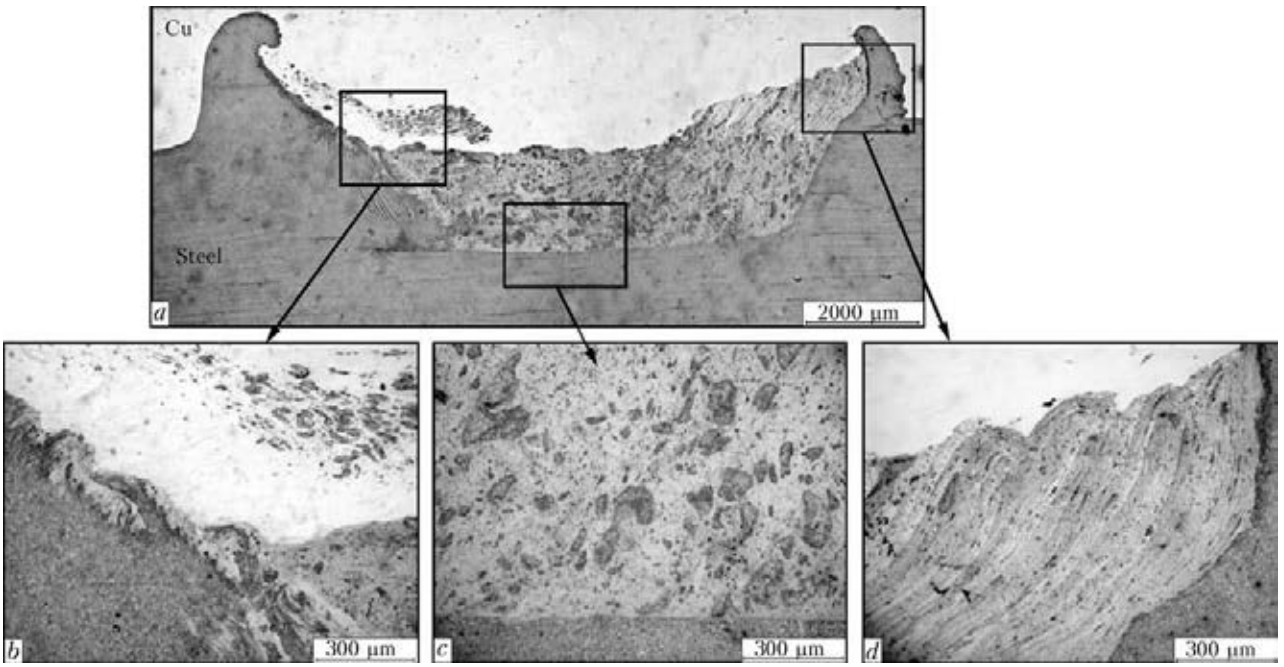

Figure 9. Cross-sectional microstructure of copper–steel welded joint produced by FSW: *a* — general view; *b*, *d* — side regions; *c* — center of copper–steel mixing zone

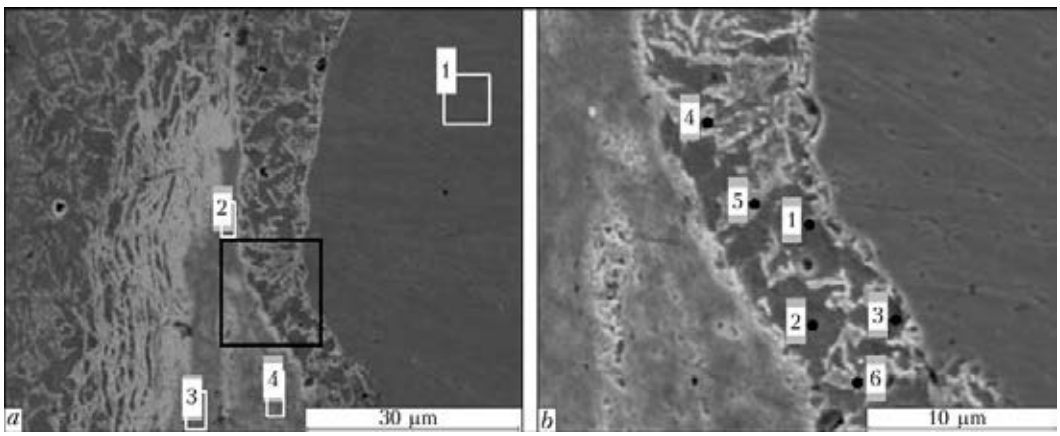

Figure 10. Microstructure of copper–steel contact zone filmed in secondary electrons

base metal. This zone microhardness is equal to 2290 ± 120, whereas for ferritic-pearlitic steel it is 2160 ± 100 MPa. As steel hardness is much higher than that of copper, no formation of classical oval nugget took place in the joint zone cross-section (see Figure 9). In its upper part joint zone consists of copper, and the lower part is a mixture of steel particles of different size in the copper matrix. Wedge-like intrusions of steel into copper to the depth of about 700–1000 μm limit the joint nugget. XRMM method was used to analyze different regions of the joint zone and determine their chemical composition (Figure 10, *a*, *b*; Table 4). As shown by investigations,

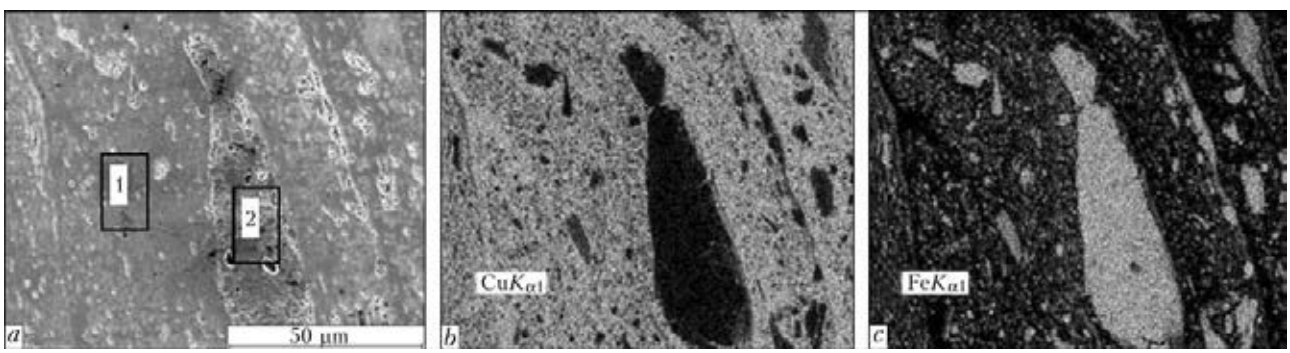

Figure 11. Copper–steel contact zone filmed in secondary electrons (*a*) and in characteristic radiation of copper (*b*) and iron (*c*)

Table 4. Composition of studied regions of copper–steel joint, wt./at.%

Studied region	Fe	Cu	Mn	Si
Acc. to Figure 10, *a*				
1	0.24/0.27	99.76/99.73	0	0
2	21.75/24.02	77.98/75.68	0.27/0.30	0
3	30.97/33.79	68.80/65.96	0.23/0.25	0
4	31.69/34.41	67.88/64.79	0.43/0.47	0.15/0.32
Acc. to Figure 10, *b*				
1	97.74/97.54	0.74/0.68	1.19/1.21	0.29/0.57
2	97.44/97.27	1.03/0.90	1.26/1.27	0.28/0.55
3	97.46/97.31	1.05/0.92	1.23/1.25	0.26/0.52
4	97.41/97.30	0.96/0.84	1.42/1.45	0.21/0.41
5	97.55/97.40	0.83/0.73	1.38/1.40	0.23/0.46
6	97.58/97.29	0.76/0.67	1.29/1.30	0.37/0.74
Acc. to Figure 11, *a*				
1	21.47/23.72	78.27/75.99	0.26/0.29	0
2	97.60/97.44	0.99/0.87	1.14/1.16	0.27/0.53

wedge-like intrusions have ferritic-pearlitic structure, and contain practically no copper. In the zone of copper to steel joint, formation of a large number of iron inclusions embedded into copper as individual bands and a mechanical mixture of copper with steel is noted. In the copper matrix a considerable quantity of iron (21.75–31.69 wt.%) was found in the form of dispersed inclusions (Table 4). Having studied boundary regions of the embedded steel band (Figure 10, *b*) we can make the assumption that processes of metal interdiffusion with solid solution formation proceed alongside copper inclusions. Results of mapping the mixing zone in Cu–steel 3 joints, which is a mechanical mixture of copper (base) and steel particles of different size, are given in Figure 11 and Table 4. Dispersed inclusions of copper are observed in the largest steel particles. No significant interdiffusion of elements is found during investigations in copper and iron characteristic radiation, but it cannot be ruled out in boundary regions. It is also established that during FSW of these metals a significant refinement of grains proceeds both in the recrystallization zone, and in the thermomechanically and heat affected zones. Conducted investigations show that metal mixing in the plastic state plays a major role in producing copper to steel welded joint by FSW process, and the role of diffusion processes is less significant.

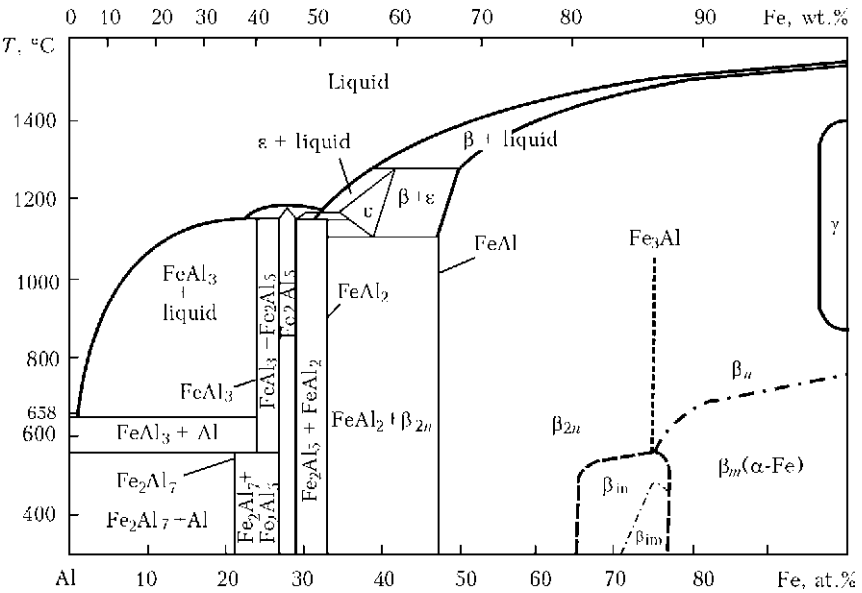

Figure 12. Constitutional diagram of Fe–Al system [19]

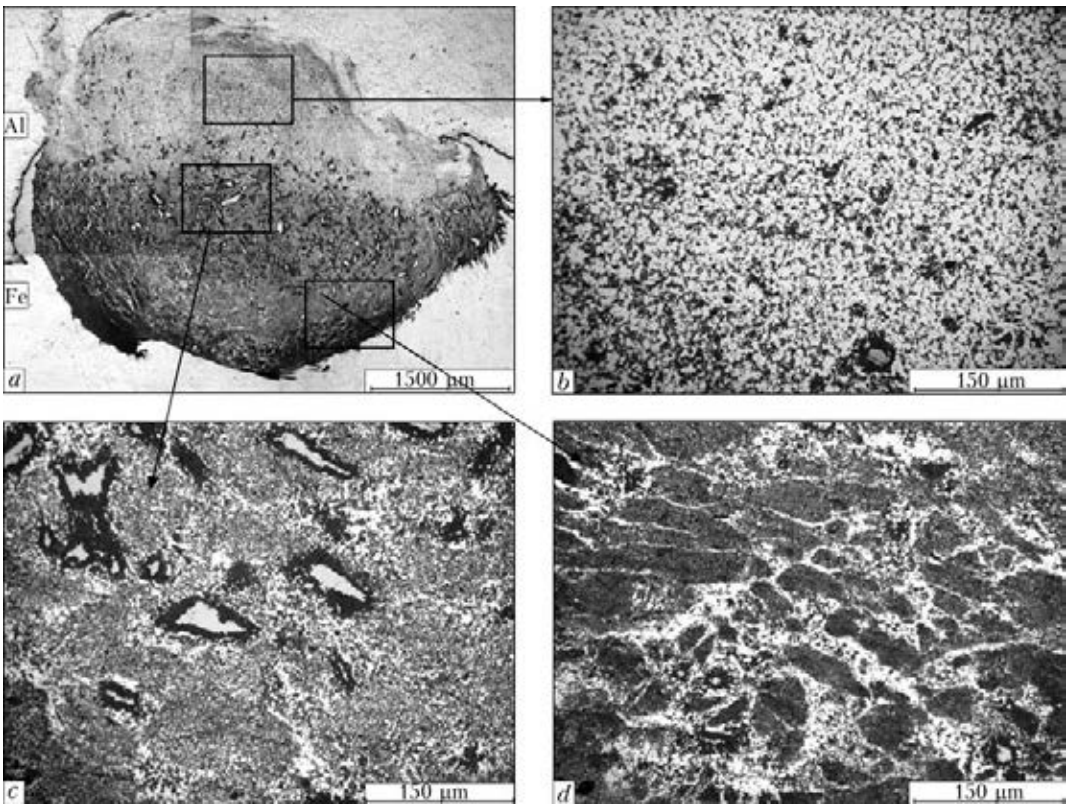

Figure 13. Cross-sectional microstructure of Fe–Al bimetal joint made by FSW: *a* — general view; *b* — upper; *c* — medium; *d* — lower part of nugget

Ability to joint dissimilar metals by FSW process in the absence of mutual solubility of elements in the solid phase was studied in the case of Fe–Al system (Figure 12). It is known from published sources that chemical interaction of aluminium and its alloys with iron, leading to irreversible formation of intermetallics in the contact zone of the two metals, prevents making sound welded joints of these metals [19, 20]. In keeping with the constitutional diagram of Fe–Al system solid solutions, intermetallic compounds and eutectics are formed. In the solid state iron solubility in aluminium is quite low, at temperatures of 225–600 °C it is in the range of 0.01–0.22 wt.%. Iron solubility in aluminium at eutectic temperature (654 °C) is equal to 0.053 wt.%, and at room temperature iron does not dissolve at all. At solidification of an alloy of aluminium with iron, $FeAl_3$ crystals form already at small amounts of iron in the structure. At up to 1.8 wt.% Fe content Al + $FeAl_3$ eutectic forms at 654 °C. At further increase of iron content (see Figure 12), chemical compounds of the following compositions form in the alloys: Fe_2Al_7, Fe_2Al_5, $FeAl_2$, FeAl and Fe_3Al with 62.9, 54.7, 49.1, 32.5 and 13.87 wt.% Al, respectively [20].

In this work an aluminium alloy and Armco-iron were joined by FSW in the modes given in Table 1. Pin tool penetrated through the aluminium alloy plate 5 mm thick to the depth of 6 mm. At FSW of these metals a nugget of 8.2 × × 5.4 mm size and a wedge-like intrusion of iron to 2 mm depth from both sides of the nugget form in the cross-section of the joint zone (Figure 13, *a*). Nugget structure is non-uniform, and consists of three zones (Figure 13, *b–d*). The nugget

Figure 14. Microstructure of upper (*a*), medium (*b*) and lower (*c*) part of nugget in Al–Fe joints, produced by FSW, filmed in back-scattered electrons (for numbers see Table 5)

Table 5. Composition of studied regions of Al–Fe joint, wt./at.%

Studied region	Fe	Al	Mn	Mg	O
Acc. to Figure 14, *a*					
1	31.27/16.91	59.06/66.12	0.28/0.15	1.41/1.76	7.97/15.06
2	27.18/14.36	62.71/68.71	0.28/0.15	2.24/2.72	7.59/14.03
3	24.83/13.09	65.53/71.49	0.68/0.36	2.26/2.74	6.70/12.32
4	0.87/0.42	92.68/92.30	0	5.65/6.22	0.79/1.33
5	2.76/1.33	90.43/90.91	0	5.59/6.20	1.22/2.06
6	4.50/2.21	89.08/90.41	0.32/0.16	5.51/6.10	0.60/1.02
7	2.11/1.02	91.99/92.10	0	5.35/5.94	0.55/0.94
8	2.98/1.45	90.28/90.89	0.37/0.18	5.76/6.43	0.62/1.05
9	4.48/2.20	89.25/90.43	0.20/0.10	5.27/5.93	0.79/1.35
Acc. to Figure 14, *b*					
1	98.69/95.87	0	0	0.26/0.57	1.05/3.56
2	90.42/81.36	8.36/15.56	0.34/0.31	0	0.88/2.78
3	23.28/12.25	66.98/72.95	1.07/0.57	2.75/3.32	5.93/10.90
4	28.67/15.14	59.31/64.83	0.37/0.20	2.61/3.17	9.03/16.65
5	1.03/0.50	93.73/94.08	0	4.47/4.98	0
6	0.50/0.24	94.56/94.30	0	4.94/5.46	0
Acc. to Figure 14, *c*					
1	99.76/99.51	0.24/0.49	0	0	0
2	21.19/11.46	74.26/83.23	0.52/0.29	4.03/5.01	0
3	25.17/13.93	70.05/80.25	0.38/0.21	4.41/5.61	0

formed primarily as a result of aluminium mass transfer, as all the zones have an aluminium matrix by XRMM data (Figure 14; Table 5). A zone with the structure of Al-based alloy with Fe_2Al_7 inclusions is located in the upper part (Figures 13, *b* and 14, *a*; Table 5). Microhardness of this zone is equal to 980–1168 MPa. Nugget middle part features the greatest non-uniformity (Figures 13, *c* and 14, *b*; Table 5). Aluminium matrix contains elongated iron particles of different size and clusters of Fe_2Al_7 and $FeAl_2$ intermetallics. At XRMM a higher content of oxygen is recorded in the studied regions, alongside Fe–Al intermetallic formation that is indicative of simultaneous formation of intermetallics and small amount of Al_2O_3 oxide. No aluminium diffusion is found in the elongated iron particles, but they have higher hardness (1360–2740 MPa), probably, as a result of deformation at plastic mixing. $FeAl_2$ intermetallic with 49 wt.% Al is in immediate vicinity, forming an iron particle fringe, and Fe_2Al_7 is chaotically located in the aluminium matrix, increasing its microhardness up to 1260–1930 MPa. It is obvious that the interdiffusion processes develop to the depth equal to thickness of formed intermetallic particles and fringes.

In the nugget zone in direct contact with iron the main structural components are Fe_2Al_7 and $FeAl_2$ aluminides, forming tongue-like intrusions into iron (Figures 13, *a*, *d* and 14, *c*). Iron aluminides are located in aluminium matrix, so that

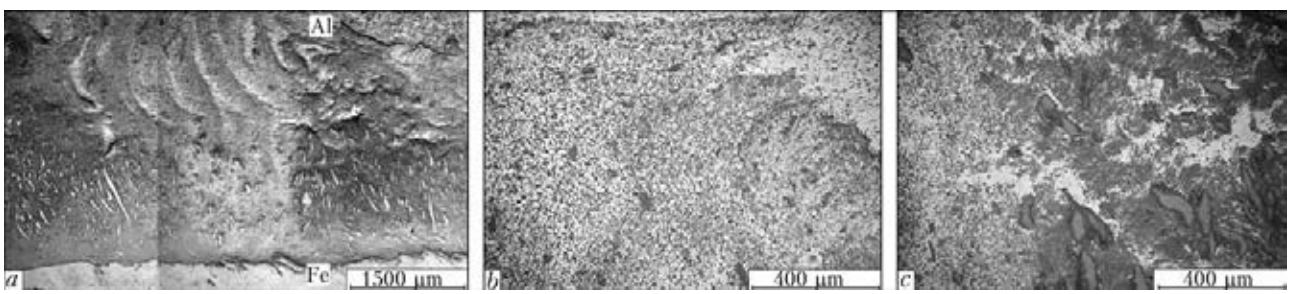

Figure 15. Microstructure of longitudinal section of Al–Fe welded joint made by FSW: *a* — general view; *b* — upper; *c* — medium region of nugget

microhardness of this zone is not high (2340–3220 MPa), compared to that of intermetallics proper (~10000 MPa). Nugget structure revealed microporosity due, obviously, to intermetallic phase formation (see Figure 14 and Table 5). By XRMM data no element interdiffusion was recorded in the aluminium alloy and in iron at 10–15 μm distance from the nugget.

When studying the longitudinal section of the joint zone (Figure 15), it was found to be continuous, without defects and having a wave-like nature, varying between 3 and 7 mm in width. Its structure consists of regions similar to the above-described regions of this welded joint cross-section.

Investigation of Al–Fe joint showed that mechanical mixing with formation of $FeAl_3$, Fe_2Al_7, $FeAl_2$ compounds proceeds during FSW process. The hardest regions of the joint zone, consisting of intermetallics in aluminium matrix, are more than 3 times softer than iron aluminides.

Conclusions

1. FSW of copper to nickel leads to interpenetration of metals to the depth of down to 3 mm. Structure refinement occurs as a result of recrystallization processes running in the bands of mechanical mixing of metals in the plastic state. Nickel regions in direct contact with copper have lower microhardness.

2. It is established that in the zone of a joint of copper to steel 3, a region of mechanical mixing of metals formed, which consists of wedge-like intrusions of steel into copper to the depth of down to 1 mm, as well as a large number of steel inclusions of different shape of 1–10 μm size. Microhardness of this mechanical mixture is 1.5 times higher than that of steel.

3. FSW of aluminium to steel resulted in formation of a joint zone of a considerable volume with aluminium penetration into iron to the depth of down to 2.5 mm. Metal interaction takes place with subsequent formation of Fe_2Al_7, $FeAl_2$ compounds. The hardest regions of the joint zone consist predominantly of iron aluminides in aluminium matrix.

4. Mechanical mixing of metals in the plastic state plays the leading role in FSW process. Role of diffusion processes is smaller. In Cu–Ni system with unlimited solubility of components in the solid state interdiffusion is found at formation of solid solution interlayers along grain boundaries to the depth of 20 μm. In Fe–Al system, when elements are not soluble in the solid state, diffusion processes proceed to the depth, equal to thickness of formed clusters of intermetallic particles and fringes down to 25 μm.

5. Conducted investigations allow recommending FSW process for welding dissimilar metals, having different solubility in the solid state, as well as for making bimetal joints.

1. Thomas, W.M., Nicholas, E.D., Needam, J.C. et al. *Friction stir butt welding*. Pat. 9125978.8 GB. Publ. Oct. 1995.
2. Vill, V.I. (1970) *Friction welding of metals*. Leningrad: Mashinostroenie.
3. Lebedev, V.K., Chernenko, I.A., Mikhalsky, R. et al. (1987) *Friction welding*: Refer. Book. Leningrad: Mashinostroenie.
4. Mishraa, R.S., Ma, Z.Y. (2005) Friction stir welding and processing. *Mater. Sci. and Eng.*, **50**, 1–78.
5. Eriksson, L.G., Larsson, R. (2003) Rotation stir welding: Research and new fields of application. *Tekhnologiya Mashinostroeniya*, **6**, 81–84.
6. Lyudmirsky, Yu.G., Kotlyshev, R.R. (2010) Friction stir welding of aluminium alloys in building industry. *Nauchn. Vestnik VGASU. Stroitelstvo i Arkhitektura*, **3**, 15–22.
7. Nikityuk, Yu.N., Grigorenko, G.M., Zelenin, V.I. et al. (2013) Technology of reconditioning repair of slab moulds of continuous-casting machine by friction stir hardfacing. *Sovr. Elektrometallurgiya*, **3**, 51–55.
8. Watanabe, H., Takayama, H., Yanagisawa, A. (2006) Joining of aluminum alloy to steel by friction stir welding. *J. Mater. Proc. Technol.*, **178**, 342–349.
9. Lee, W.-B., Schmuecker, M., Mercardo, U.A. et al. (2006) Interfacial reaction in steel-aluminum joints made by friction stir welding. *Scripta Mater.*, **55**, 355–358.
10. Kostka, A., Coelho, R.S., dos Santos, J. et al. (2000) Microstructure of friction stir welding of aluminium alloy to magnesium alloy. *Ibid.*, **66**, 953–956.
11. Kwon, Y.J., Shigematsu, I., Saito, N. (2008) Dissimilar friction stir welding between magnesium and aluminium alloys. *Materials Letters*, **62**, 3827–3829.
12. Xue, P., Ni, D.R., Wang, D. et al. (2011) Effect of friction stir welding parameters on the microstructure and mechanical properties of the dissimilar Al–Cu joints. *Mater. Sci. and Eng.*, **528**, 4683–4689.
13. Saeida, T., Abdollah-Zadehb, A., Sazgarib, B. (2010) Weldability and mechanical properties of dissimilar aluminum-copper lap joints made by friction stir welding. *J. Alloys and Compounds*, **490**, 652–655.
14. Grigorenko, G.M., Zelenin, V.I., Kavunenko, P.M. et al. (2012) Stir friction hardfacing by nickel of copper mould walls of continuous-casting machines. In: *Problems of resource and service safety of structures, constructions and machines*. Kyiv: PWI, 369–372.
15. Poleshchuk, M.A., Grygorenko, G.M., Kavunenko, P.M. et al. *Insert of working tool of machine for friction stir welding and surfacing*. Pat. 25394 for a design, Ukraine. Publ. 10.09.2013.
16. Beckert, M.K., Clemm, H. (1988) *Methods of metallographic etching*: Refer. Book. Moscow: Metallurgiya.
17. Hansen, M., Anderko, K. (1962) *Structure of binary alloys*. Vol. 1, 2. Moscow: Metallurgizdat.
18. (1979) *Binary and multicomponent systems on copper base*: Refer. Book. Ed. by N.Kh. Abrikosov. Moscow: Nauka.
19. Rabkin, D.M., Ryabov, V.R., Gurevich, S.M. (1975) *Welding of dissimilar metals*. Kiev: Tekhnika.
20. Ryabov, V.R., Rabkin, D.M., Kurochko, R.S. et al. (1984) *Welding of dissimilar metals and alloys*. Moscow: Mashinostroenie.

Received 02.10.2013